Available online at www.sciencedirect.com
SCIENCE DIRECT®
Journal of Molecular Graphics and Modelling 23 (2005) 297–303
Journal of Molecular Graphics and Modelling
www.elsevier.com/locate/JMGM

Homology modelling of RNA polymerase and associated transcription factors from *Bacillus subtilis*

Iain J.A. MacDougall, Peter J. Lewis, Renate Griffith*

School of Environmental and Life Sciences, The University of Newcastle, Biology Building, Callaghan, NSW 2308, Australia

Received 25 June 2004; received in revised form 29 September 2004; accepted 11 October 2004
Available online 21 November 2004

Abstract

RNA polymerase (RNAP) is the central enzyme of transcription and requires interaction with transcription factors in vivo for correct processivity. Both the transcription initiation complex and the ternary elongation complex are stabilised by and require protein–protein interactions between the various components involved. These interactions may form the basis for rational design of small peptide mimics of one or more proteins involved in order to inhibit protein–protein interactions and thus transcription. Here, we present homology models of the model Gram positive organism *Bacillus subtilis* RNA polymerase in the core and holoenzyme forms. Interactions between RNA polymerase and the transcription factor σ^A were investigated in order to design peptide mimics of the major interactions.

Keywords: Homology modelling; RNA polymerase; Protein–protein interactions; Peptide mimic; σ-Factor

1. Introduction

RNA polymerase (RNAP) is the central enzyme responsible for transcription. In *Bacillus subtilis*, core RNAP has the subunit makeup $\alpha_2\beta\beta'$ along with the poorly conserved and loosely associated ω and δ proteins. Unable to transcribe intact DNA by itself, core RNAP requires interaction with one of a family of proteins known as σ-factors in order to initiate transcription [1]. When σ is complexed with core RNAP the structure is referred to as the holoenzyme (HE). In *B. subtilis*, the primary σ-factor, σ^A, is responsible for recognising promoter elements of DNA and initiating the majority of transcription during exponential growth [2]. HE requires interaction with other transcription factors such as the Gre proteins and Nus factors to maintain fidelity and ensure appropriate termination of transcription.

A number of high-resolution structures for RNAP core and HE from *Thermus aquaticus* and *Thermus thermophilus* have recently been solved [3–5]. These structures give valuable insights into the structure and function of RNAP, and the information can be applied to many species due to large-scale similarities between the structures (reviewed in [6,7]). These extremophile organisms are phylogenetically removed from *B. subtilis*, and although certain regions such as the active site motif NADFDGD [8] are extremely well conserved, other areas such as protein–protein interaction surfaces are not. The interaction between σ-factors and RNAP is crucial for the appropriate initiation of transcription. In *B. subtilis* there are 17 σ-factors which play important roles in differential gene expression under varying cellular conditions such as sporulation and response to environmental stresses (reviewed in [9]). *B. subtilis* is harmless, but closely related to significant pathogens such as *Bacillus anthracis* and *Staphylococcus aureus* and is widely used as a model Gram positive experimental system. The models of RNAP and associated transcription factors presented here could therefore be used as a basis for an experimental assay in *B. subtilis* with direct relevance to pathogenic species. Of particular interest to this study was the interaction in *B. subtilis* between σ^A and RNAP.

Mutation analysis indicates that domain 2.1 of the sporulation-dependent σ^E (highly similar to σ^A in this region) is required in *B. subtilis* for high-affinity binding of

* Corresponding author. Tel.: + 61 249216990; fax: +61 249216923.
E-mail address: Renate.Griffith@newcastle.edu.au (R. Griffith).

1093-3263/$ – see front matter © 2004 Elsevier Inc. All rights reserved.
doi:10.1016/j.jmgm.2004.10.001

σ-factors to core [10] and the *T. thermophilus* HE crystal structure indicates contacts between this, the adjacent regions 2.2 and 2.3 of σ^{70} (equivalent to *B. subtilis* σ^{A}) and a helix-turn-helix (HtH) motif of the β′ subunit [3]. This motif is solvent-exposed in the core structure and as such would be an accessible target for inhibition.

This interaction has been implicated as the major binding interface important for maintaining appropriate contacts between RNAP, σ-factor and DNA during the initiation phase of transcription and during σ-factor dissociation (reviewed in [7]). As such, disruption of this interaction may lead to inhibition of transcription, with obvious antimicrobial benefits. Although transcription is of central importance to cell survival, few antimicrobial agents have been directed towards the RNAP complex. Rifampicin and streptolydigin are well-known small-molecule inhibitors of RNAP, as is the short peptide inhibitor Microcin J25 (MccJ25) [11–14]. MccJ25 acts by binding within the nucleotide entry channel and blocking the path of the nucleotide triphosphates to the active site [15]. Due to the size of RNAP and the number of protein–protein interactions central to RNAP function, there are a wide variety of targets for potential inhibition by small peptides, which don't directly involve inhibition of the polymerase activity. It is not unreasonable to expect that small peptides may competitively bind regions of RNAP in preference over transcription factors.

Many systems such as flagellar biosynthesis in *Salmonella typhimurium* (reviewed in [16]) and sporulation inhibition in *B. subtilis* [17] require the presence of anti-σ factors. With particular relevance to this study, the anti-σ protein AsiA has been shown to directly compete with the β flap for binding to σ in order to disrupt the interaction and inhibit transcription [18].

Here, we present models of *B. subtilis* RNAP in core and HE form with particular emphasis on the protein–protein interactions between RNAP and the transcription factor σ^{A}. These interactions were investigated with a view to designing small peptide mimics to act as inhibitors of protein–protein interactions.

2. Methods

2.1. Sequence alignments

Sequences for *B. subtilis* proteins were obtained from the SubtiList database (genolist.pasteur.fr/SubtiList). Coordinates of crystal structures were obtained from the Protein DataBank (PDB) [19]. Sequence alignments were created with ClustalW version 1.74 [20]. Alignments were further refined manually with Swiss-PDBViewer version 3.7 [21–23] to accommodate non-conserved loop regions. Alignments were created with each of the *B. subtilis* proteins against corresponding crystal structures acquired from the PDB prior to modelling.

2.2. Homology modelling

All homology models were constructed using Swiss-PDBViewer version 3.7 [21–23]. Homology models of *B. subtilis* RNAP core subunits were based on the crystal structure for *T. aquaticus* RNAP (PDB code 1I6V). The subunits of *B. subtilis* and *T. aquaticus* RNAP other than the non-essential ω share between 41 and 55% identity and between 57 and 70% similarity of sequence. Homology models of *B. subtilis* RNAP HE subunits including σ^{A} were based on the crystal structure for *T. thermophilus* RNAP (PDB code 1IW7). The subunits of *B. subtilis* and *T. thermophilus* RNAP other than the non-essential ω share between 43 and 55% identity and between 59 and 70% similarity of sequence.

2.3. Model and template refinement

Homology models were imported into Sybyl6.9 (Tripos Inc., St. Louis, MO, USA) for refinement. Atoms types were checked, all hydrogens were added and partial charges were assigned from a library (Kollmann_all). Explicit water molecules or implicit solvation models were not used in this work. Initially, backbone atoms were constrained and the structures minimised with the Steepest Descent and Powell algorithms as implemented in the Tripos forcefield. Structures were then minimised without constraints using the Steepest Descent and Powell algorithms until the maximum derivative was less than 0.05 kJ/(mol Å). The Tripos software was unable to minimise the β and β′ subunits due to their size. All subunits were exported to DSModeling 1.1 (Accelrys, San Diego, CA, USA) for further minimisation using the CHARMm forcefield. The structures were minimised without constraint using the Steepest Descent and Powell algorithms until the maximum derivative was less than 0.01 kJ/(mol Å). Subunits of the crystal structure templates 1I6V and 1IW7 were treated in the same manner as described above.

2.4. Protein complex assembly

Structures of *B. subtilis* RNAP in core and holoenzyme form were constructed from the homology models of the individual subunits minimised in DSModeling 1.1. Each minimised subunit was superimposed over the corresponding subunit of the crystal structure until the complete structure was built. The template crystal structure was subsequently removed leaving a rough model of *B. subtilis* RNAP.

2.5. Evaluation of models

Backbone conformations of the minimised *B. subtilis* proteins were evaluated via the Ramachandran plot from PROCHECK [24] at the appropriate resolutions and compared to the corresponding crystal structures. Root mean square deviation (RMSD) values were calculated for

each of the minimised homology models compared to the template structure. In order to investigate regions of greatest movement within the proteins before and after minimisation, the structures were subjected to distance difference matrix (DDM) analysis using ProFlex [25]. Subunits of *B. subtilis* core and HE complexes were also subjected to RMSD and DDM analysis to detect differences between the structural forms.

3. Results and discussion

3.1. Homology modelling of B. subtilis proteins

The sequence identity between conserved *B. subtilis* RNAP subunits and their template sequences ranges from 41–55% (Table 1). The models for *B. subtilis* HE subunits were based on the 2.6 Å structure of RNAP HE from *T. thermophilus* (1IW7; [3]). Global topology for the subunits is generally quite similar between the homology models and the templates. In the β′ subunit of *T. thermophilus* there is a non-conserved domain consisting of 288 amino acids which is not present in the *B. subtilis* protein. The corresponding region in *B. subtilis* instead consists of a 5aa loop with extended secondary structure.

Models for the core subunits were based on the 3.3 Å structure of RNAP core from *T. aquaticus* (1I6V; [4]). The overall topology of the subunits is again quite similar to the crystal structures, however, in the core template there is no large insert in the β′ subunit.

RMSD values were calculated comparing the minimised *B. subtilis* models to the unminimised templates (Table 1). It was found that comparison to minimised templates did not greatly affect the RMSD values, the RMSD of HE β subunits changed from 2.62 to 2.70 and β′ changed from 3.99 to 3.86 upon minimisation of the templates. The larger RMSD values are indicative of either large structures such as the β and β′ subunits or of structures with poor homology to the template, such as the ω subunits.

3.2. Quality of the models

Model quality was assessed using a variety of validation tools implemented by the PROCHECK program [24]. Ramachandran plot analysis indicated that 93–99% of backbone dihedral angles of all subunits of *B. subtilis* HE lay in the allowed regions, compared with 100% for the 2.6 Å template crystal structure. Similar analyses for *B. subtilis* core subunits indicated that 96–97% of backbone dihedral angles lay in the allowed regions, compared to 93–98% for the 3.3 Å template crystal structure. RMSDs were also calculated for the structures before and after minimisation to show there were no gross movements which would indicate that the templates used were not suitable. These values for core subunits ranged from 1.42 to 2.71 Å and for HE subunits ranged from 1.12 to 2.42 Å. While the RMSD analysis gives an impression of the overall difference between two structures it is not useful in detecting the particular regions of greatest movement. ProFlex [25] was used to determine regions of greatest movement within the proteins upon minimisation. This analysis showed that the regions of greatest movement (all less than 5 Å for C_α atoms) within the α subunit are located at both termini of the model.

3.3. RNA polymerase model construction

Models of *B. subtilis* RNAP in core and HE form were constructed from the homology models of their respective subunits. The core model consists of α1, α2, β, β′ and ω subunits; HE also contains the σ^A subunit. *B. subtilis* RNAP models were constructed by manually overlaying the minimised homology models of each individual subunit onto the corresponding crystal structure. The template was then removed, leaving structures representative of *B. subtilis* RNAP in core and HE forms.

In order to visually verify the accuracy of the overall structures, data pertaining to transcription factor interaction sites [26,27] were mapped onto the *B. subtilis* core and HE models. On the core model, residues shown to be within 4 Å of GreB in the crystal structure [27] were shown to lie within and around the lip of the secondary, or nucleotide-entry channel (displayed in red in Fig. 1A). This channel allows the entry of single nucleotide triphosphates into the structure towards the active site (Fig. 1A, orange arrow). The lip of this channel features a solvent-exposed, so-called secondary channel rim helix-turn-helix motif [27] (sc-rim helices, lower portion of Fig. 1A) that may play a role in stabilising the interaction between RNAP and Gre factors. Fig. 1A also shows the solvent-accessible active site NADFDGD motif of

Table 1
Summary of sequence and structural similarities between homology models of *B. subtilis* proteins and their corresponding crystal structures. RMSD values were calculated in Sybyl6.9 for all backbone atoms of minimised structures

Subunit	*B. subtilis* HE vs. template			*B. subtilis* core vs. template			HE vs. core	
	Identity	Similarity	RMSD	Identity	Similarity	RMSD	*B. subtilis* (RMSD)	Templates (RMSD)
Alpha	41	57	2.31	43	59	1.42	2.31	2.39
Beta	55	70	2.62	55	70	N.D.	N.D.	4.36
Betaprime	48	64	3.99	48	64	2.90	7.21	4.76
Omega	27	52	3.55	30	53	3.52	3.32	3.32
Sigma	54	65	3.20					

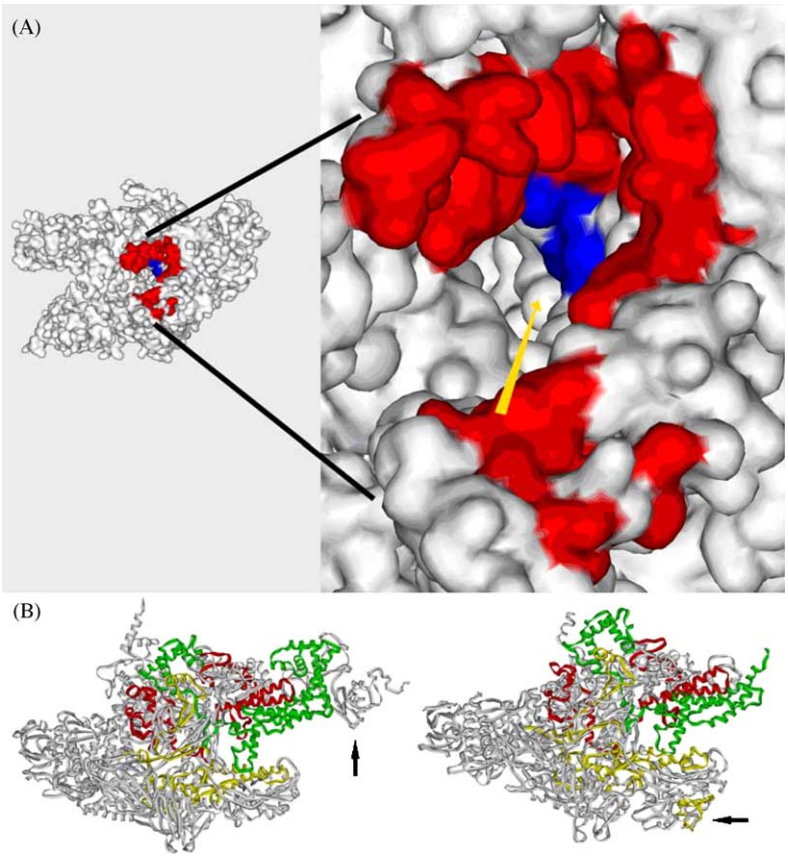

Fig. 1. A view of the core RNAP solvent-exposed surface showing the entrance to the secondary channel. Entering nucleotide triphosphates follow the path of the orange arrow. Residues of β and β′ highlighted in red were implicated in interacting with the transcription factor GreB from the crystal structure [27]. The active site motif NADFDGD is highlighted in blue and can be seen to be solvent-exposed. B: Visual comparison of data from footprinting studies [26] projected onto *T. thermophilus* (left) and *B. subtilis* (right) HE structures. In both structures α, β, β′ and ω are coloured grey and $\sigma^{A/70}$ is coloured green. Regions of β and β′ implicated in interacting with transcription factors by [26] are coloured yellow and red, respectively. Black arrows indicate non-conserved regions of *T. thermophilus* β′ (left) and *B. subtilis* β (right).

the β subunit (shown in blue). The structure of core was further seen to correlate with the literature as residues of the β and β′ subunits, which make up part of the upstream binding site [28–29], were shown to be in an appropriate position within the structure (data not shown).

Low-resolution footprinting data describing the interaction of σ^{70} and Nus factors with *Escherichia coli* RNAP [26] was displayed on the *B. subtilis* HE structure and compared to the same data mapped onto the template crystal structure (Fig. 1B). This figure indicates that the pattern of highlighted residues is very similar for the homology-based HE model and the crystal structure. The large-scale structures are also similar except for two regions in the β and β′ subunits which are not conserved between the two species (Fig. 1B, black arrows). The non-conserved region of *B. subtilis* β was modelled automatically by SWISS-MODEL [21–23].

RMSD values were calculated for the α, β, β′ and ω subunits between the core and HE models to detect large-scale differences (Table 1). The comparatively larger RMSD value for the β′ subunit of 7.21 indicates that this subunit undergoes the most conformational change between the core and HE forms. DDM analysis of the β′ subunit indicated differences in the positions of C_α atoms of more than 15 Å in the N-terminal 85 residues, residues 110–165 and residues 515–590. Fig. 2 shows the DDM for the β′ subunit with the HtH motif of interest indicated. Regions are coloured according to the magnitude of difference between structures. The HtH motif was found to move 2–5 Å between core and HE forms.

3.4. β′/σ^A interface and inhibitor design

Of particular interest to this study is the interaction between the β′ subunit of RNAP and σ^A. In our model, the flexible predominantly negatively-charged domain 3.2 of σ^A is situated in the RNA exit channel where it is able to interact with the transcript during the initiation phase. Domains 2.1, 2.2 and 2.3 were determined to lie close to the HtH motif of β′ formed by residues 253–297, as was expected. σ^A domain 1.1 was not included in the *B. subtilis* model, and, as such, no observations can be made regarding its interaction with β′. FRET studies have shown region 1.1 to be quite flexible while in complex with RNAP [30] and as a result it has not been resolved in crystal structures.

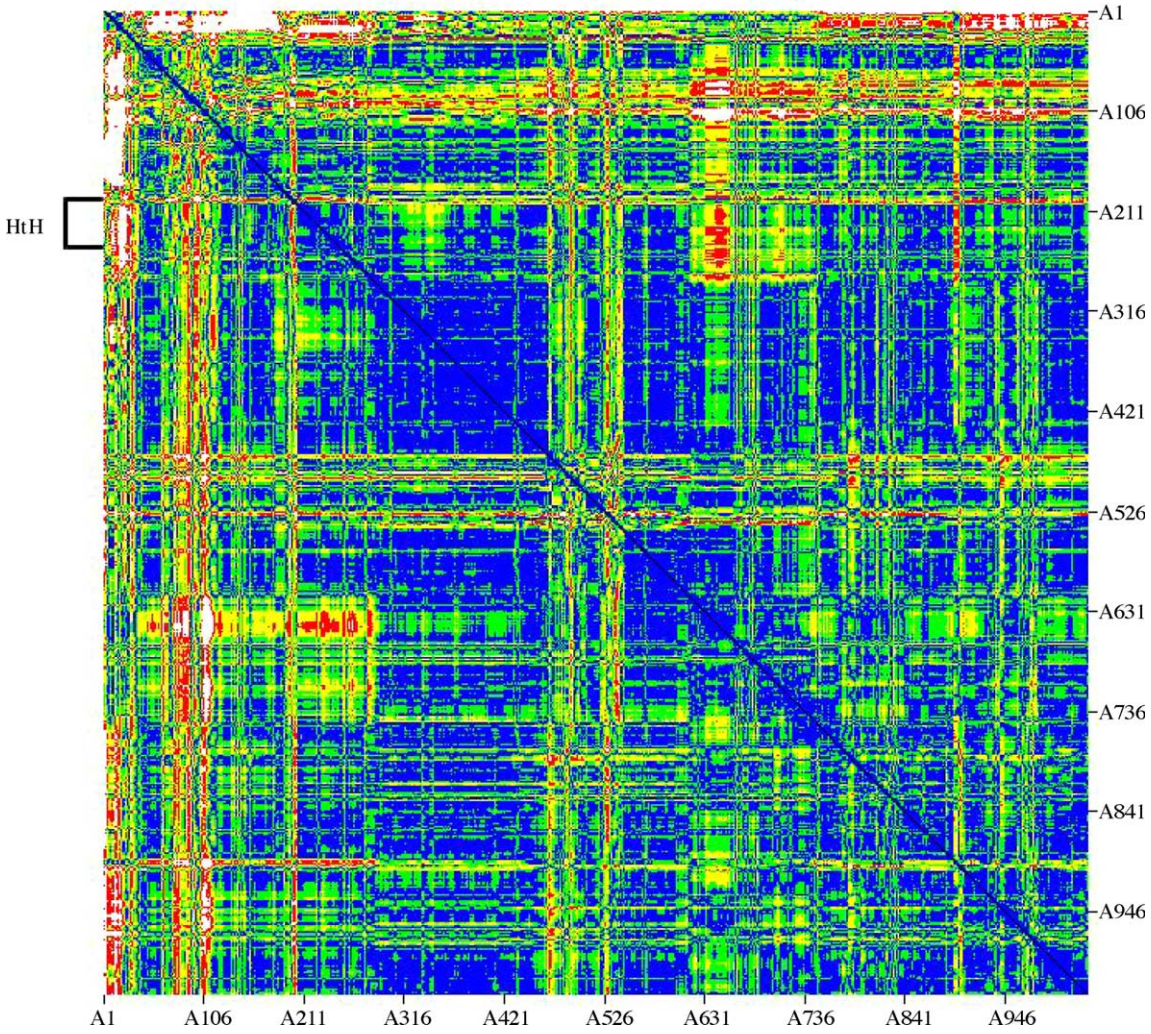

Fig. 2. Difference distance matrix for the C_α atoms of the β′ subunit of *B. subtilis* core and HE. Values on each axis refer to residue numbers. Colour coding corresponds to the following movements, blue: 0.0–2.0 Å; green: 2.0–5.0 Å; yellow: 5.0–10.0 Å; red: 10.0–15.0 Å; white: >15.0 Å. The β′ helix-turn-helix motif of interest is indicated.

The protein–protein interaction interface between domain 2.2 of σ^A and the HtH region of β′ has been identified as being the major interaction between the two proteins (Fig. 3; [3]). Visual analysis of the core and holoenzyme structures indicate that this HtH motif is solvent-exposed in the absence of σ^A. As other interactions between β′ and σ^A are either weaker or not solvent-exposed it was decided that this interaction face would be a good initial choice for designing a peptide mimic. As it was not possible to minimise the entire HE structure due to its size, the σ^A and β′ subunits alone were subjected to minimisation with the rest of the structure constrained.

The predominant stabilising interaction within this interface was found to result from a network of charge-reinforced hydrogen bonding between five residues: σD162, σE166, β′N263, β′R264 and β′R267 (Fig. 3C). The distances between the closest charged oxygens of σ^A residues and the proximal hydrogens of the β′ residues are between 1.89 Å and 1.98 Å, close to the expected value of 1.8–1.9 Å for these interactions as calculated with Spartan'02 (Wavefunction Inc., Irvine, CA, USA). A hydrophobic patch was observed on the β′ HtH, facing domain 2.2 of σ^A, consisting of the residues L271, L274, P277 and I280 (Fig. 3B). As this region would be solvent-exposed while RNAP is in core form, it can be expected that this region of β′ preferentially binds hydrophobic regions of peptides. Indeed, two large hydrophobic methionine residues of σ^A domain 2.2 are situated proximal to this hydrophobic pocket (not shown).

When designing inhibitory peptides based on σ^A domain 2.2, one must take into account the helical propensity (P_α) of the sequence. The P_α of the direct mimic (exact sequence of the interacting helix of σ^A domain 2.2, shown in red in Fig. 3) was calculated at an average of 1.07 per residue according to the Chou–Fasman helix propensities for amino acids [31]. In order to increase the helical propensity of the mimic, non-interacting residues may be substituted with alanines, which have a high P_α and are classified as helix-favouring.

Table 2
Peptide inhibitor sequences

	Peptide sequence
Direct mimic	ASP-LEU-ILE-HIS-GLU-GLY-ASN-MET-GLY-LEU-MET
Altered mimic example	GLU-ALA-ALA-MET-GLU-ALA-ASN-ILE-ALA-ALA-ILE
Randomised control	MET-HIS-LEU-ASN-GLY-GLU-ILE-GLY-MET-ASP-LEU

The two major structural features that would need to be exploited are the charge-reinforced hydrogen bonding interactions and the hydrophobic patch. The two σ^A residues involved in the H-bond network, σD162 and σE166, may be substituted with any combination of aspartic and glutamic acids in order to explore and potentially improve these interactions. While the charge reinforced hydrogen bonding at the N-terminus of σ^A domain 2.2 appears to be fairly strong already, it may be possible to improve the hydrophobic interactions at the C-terminal end. The methionine residues may be replaced with branched hydrophobic residues such as valine or isoleucine to potentially increase the hydrophobic patch interactions. The positively charged σH165 lies within 2.63 and 2.37 Å of two hydrophobic β′ residues, β′I280 and β′M287. In order to expand the hydrophobic patch interactions σH165 could be replaced by a hydrophobic residue such as methionine, which also has a high P_α.

Table 2 shows the sequences of the direct mimic; an example of an altered mimic with some of the modifications suggested above; and a randomised version of the direct mimic which would be used as a negative control peptide. The P_α for the altered mimic example was calculated at an average of 1.31 per residue.

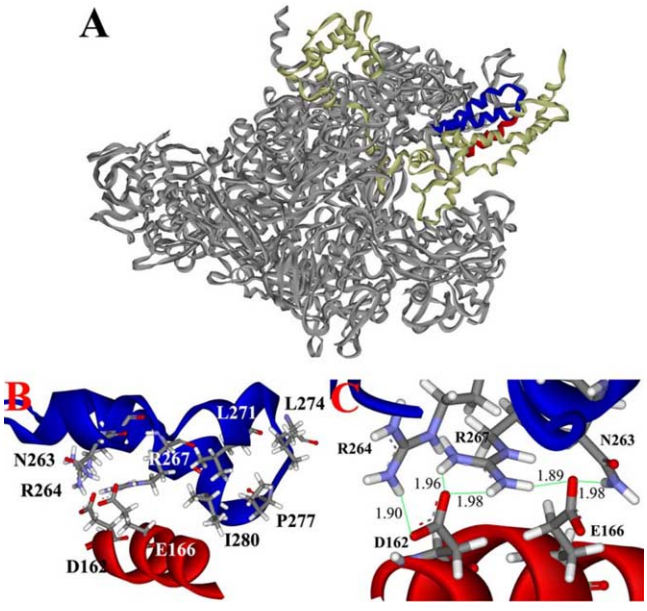

Fig. 3. The interaction interface between the β′ and σ^A subunits. (A) RNAP is coloured grey and σ^A is coloured yellow. Domain 2.2 of σ^A is coloured red and the HtH motif of β′ is coloured blue. (B) The interaction interface of interest between σ^A and β′. Residues forming the hydrophobic patch on β′ can be seen on the right side of the figure. (C) The network of charge-reinforced hydrogen bonding between σD162, σE166, β′N263, β′R264 and β′R267 (green lines).

4. Conclusions

In summary, we have shown the successful construction of RNAP protein complexes for *B. subtilis* based on homology modelling. Our structures were validated both in terms of backbone geometry and their conformity to experimental evidence. We identified the interaction between σ^A region 2.2 and a β′ HtH motif as being important to the stability of the β'/σ^A interaction. This interaction was found to involve a network of charge-reinforced H-bonds and a hydrophobic patch. Using the structures as a basis, we have been able to design small peptides which may act as mimics to a specific, essential protein–protein interaction of the holoenzyme. It is our hope that this technique may be used to exploit other interaction faces as potential sites for inhibition. Other candidates for the design of mimics include the protein–protein interactions between RNAP and Nus factors; and between RNAP and GreA. Mimics which target essential protein–protein interactions such as the one investigated here may be tested in *B. subtilis*, the biologically safe, genetically flexible, model Gram positive bacterium. These rationally-designed mimics may ultimately lead to applications for closely related, clinically relevant bacteria such as *B. anthracis* and *S. typhimurium*.

References

[1] E. Burgess, A. Travers, J. Dunn, E. Bautz, Factor stimulating transcription by RNA polymerase, Nature 221 (1969) 43–46.
[2] C. Gross, C. Chan, A. Dombroski, T. Gruber, M. Sharp, J. Tupy, B. Young, The functional and regulatory roles of sigma factors in transcription, Cold. Spring Harb. Symp. Quant. Biol. 63 (1998) 141–155.
[3] D. Vassylyev, S.-I. Sekine, O. Laptenko, J. Lee, M. Vassylyeva, S. Borukhov, S. Yokohama, Crystal structure of a bacterial RNA polymerase holoenzyme at 2.6 Å resolution, Nature 752 (2002) 1–9.
[4] G. Zhang, E. Campbell, L. Minakhin, C. Richter, K. Severinov, S.A. Darst, Crystal structure of *Thermus aquaticus* core RNA polymerase at 3.3 Å resolution, Cell 98 (1999) 811–824.
[5] K. Murakami, S. Masuda, S.A. Darst, Structural basis of transcription initiation: RNA polymerase holoenzyme at 4 Å resolution, Science 296 (2002) 1280–1284.

[6] P. Cramer, Multisubunit RNA polymerases, Curr. Opin. Struct. Biol. 12 (2002) 89–97.
[7] K. Murakami, S. Darst, Bacterial RNA polymerases: the wholo story, Curr. Opin. Struct. Biol. 13 (2003) 31–39.
[8] E. Zaychikov, E. Martin, L. Denissova, M. Kozlov, V. Markovtsov, M. Kashlev, H. Heumann, A. Goldfarb, A. Mustaev, Mapping of catalytic residues in the RNA polymerase active center, Science 273 (1996) 107–109.
[9] J. Helmann, C. Moran, RNA polymerase and sigma factors, in: A.L. Sonenshein, J.A. Hoch, R. Losick (Eds.), *Bacillus subtilis* and its Closest Relatives from Genes to Cells, ASM Press, Washington. DC, 2002, pp. 289–312.
[10] M. Shuler, K. Tatti, K. Wade, C. Moran, A single amino acid substitution in σ^E affects its ability to bind core RNA polymerase, J. Bacteriol. 177 (1995) 3687–3694.
[11] E.A. Campbell, N. Korzheva, A. Mustaev, K. Murakami, S. Nair, A. Goldfarb, S.A. Darst, Structural mechanism for rifampicin inhibition of bacterial RNA polymerase, Cell 104 (2001) 901–912.
[12] L.M. Heisler, K. Suzuki, R. Landick, C.A. Gross, Four contiguous amino acids define the target for streptolydigin resistance in the β subunit of *Escherichia coli* RNA polymerase, J. Biol. Chem. 268 (1993) 25369–25375.
[13] K. Severinov, D. Markov, E. Severinova, V. Nikiforov, R. Landick, S.A. Darst, A. Goldfarb, Streptolydigin-resistant mutants in an evolutionarily conserved region of the β subunit of *Escherichia coli* RNA polymerase, J. Biol. Chem. 270 (1995) 23926–23929.
[14] J. Yuzenkova, M. Delgado, S. Nechaev, D. Savalia, V. Epshtein, I. Artsimovich, R.A. Mooney, R. Landick, R.N. Farias, R. Salomon, K. Severinov, Mutations of bacterial RNA polymerase leading to resistance to microcin J25, J. Biol. Chem. 277 (2002) 50867–50875.
[15] J. Mukhopadhyay, E. Sineva, J. Knight, R.M. Levy, R.H. Ebright, Antibacterial peptide microcin J25 inhibits transcription by binding within and obstructing the RNA polymerase secondary channel, Mol. Cell. 14 (2004) 739–751.
[16] P. Aldridge, K.T. Hughes, Regulation of flagellar assembly, Curr. Opin. Microbiol. 5 (2002) 160–165.
[17] J. Clarkson, I.D. Campbell, M.D. Yudkin, Physical evidence for the induced release of the *Bacillus subtilis* transcription factor, σ^F, from its inhibitory complex, J. Mol. Biol. 340 (2004) 203–209.
[18] B.D. Gregory, B.E. Nickels, S.J. Garrity, E. Severinova, L. Minakhin, R.J. Bieber Urbauer, J.L. Urbauer, T. Heyduk, K. Severinov, A. Hochschild, A regulator that inhibits transcription by targeting an intersubunit interaction of the RNA polymerase holoenzyme, Proc. Natl. Acad. Sci. U.S.A. 101 (2004) 4554–4559.
[19] H.M. Berman, J. Westbrook, Z. Feng, G. Gilliland, T.N. Bhat, H. Weissig, I.N. Shindyalov, P.E. Bourne, The protein data bank, Nucleic Acids Res. 28 (2000) 235–242.
[20] D.G. Higgins, T.J. Gibson, Using CLUSTAL for multiple sequence alignments, Methods Enzymol. 266 (1996) 383–402.
[21] N. Geux, M. Peitsch, SWISS-MODEL and the Swiss-PdbViewer: an environment for comparative protein modelling, Electrophoresis 18 (1997) 2714–2723.
[22] M. Peitsch, Protein modeling by E-mail, Bio/Technology 13 (1995) 658–660.
[23] M. Peitsch, ProMod Swiss-Model: internet-based tools for automated comparative protein modelling, Biochem. Soc. Trans. 24 (1996) 274–279.
[24] R.A. Laskowski, M.W. MacArthur, D.S. Moss, J.M. Thornton, PROCHECK: a program to check the stereochemical quality of protein structures, J. Appl. Cryst. 26 (1993) 283–291.
[25] P.A. Keller, S.P. Leach, T.T.T. Luu, S.J. Titmuss, R. Griffith, Development of computational and graphical tools for analysis of movement and flexibility in large molecules, J. Mol. Graph. Model. 18 (2000) 235–241.
[26] S. Traviglia, S. Datwyler, D. Yan, A. Ishihama, C. Meares, targeted protein footprinting: where different transcription factors bind to RNA polymerase, Biochemistry 38 (1999) 15774–15778.
[27] N. Opalka, M. Chlenov, P. Chacon, W.J. Rice, W. Wriggers, S.A. Darst, Structure and function of the transcription elongation factor GreB bound to bacterial RNA polymerase, Cell 114 (2003) 335–345.
[28] K. Liu, Y. Zhang, K. Severinov, A. Das, M. Hanna, Role of *Escherichia coli* RNA polymerase alpha subunit in modulation of pausing, termination and anti-termination by the transcription factor NusA, EMBO J. 15 (1996) 150–161.
[29] E. Nudler, Transcription elongation: structural basis and mechanisms, J. Mol. Biol. 288 (1999) 1–12.
[30] V. Mekler, E. Kortkhonjia, J. Mukhopadhyay, J. Knight, A. Revyakin, A. Kapanidis, W. Niu, Y. Ebright, R. Levy, R. Ebright, Structural organisation of bacterial RNA polymerase holoenzyme and the RNA polymerase-promoter open complex, Cell 108 (2002) 599–614.
[31] P.Y. Chou, G.D. Fasman, Empirical predictions of protein conformation, Annu. Rev. Biochem. 47 (1978) 251–276.